

Macro-scale fast flow and magnetic field generation in 2-temperature relativistic electron-ion plasmas of astrophysical objects

K. Kotorashvili¹ • N.L. Shatashvili^{1,2,*}

Abstract We have shown the simultaneous generation of macro-scale fast flows and strong magnetic fields in the 2-temperature relativistic electron-ion plasmas of astrophysical objects due to Unified Reverse Dynamo/Dynamo mechanism. The resulting dynamical magnetic field amplification and/or flow acceleration is directly proportional to the initial turbulent kinetic/magnetic (magnetic) energy; the process is very sensitive to relativistically hot electron-ion fraction temperature and magneto-fluid coupling. It is shown, that for realistic physical parameters of White Dwarfs accreting hot astrophysical flow / Binary systems there always exists such a real solution of dispersion relation for which the formation of dispersive strong super-Alfvénic macro-scale flow/outflow with Alfvén Mach number $> 10^6$ and/or generation of super-strong magnetic fields is guaranteed.

Keywords stars: evolution; stars: binaries; stars: white dwarfs; stars: winds, outflows; galaxies: jets; plasmas

1 Introduction

Multi-temperature composite systems are often met in various astrophysical settings, e.g. a highly degenerate White Dwarf (WD) plasma co-existing with a classical hot accreting astrophysical flow. WDs

- interesting representatives of compact astrophysical objects - comprise up to 98% of the end state of all stars (Winget & Kepler 2008; Camenzind 2007; Külebi et al 2009; Kepler et al 2013). It is considered that accreting WDs (AWD) are featuring global magnetic structures with field strengths (1 – 1000) MG (Koester & Chanmugam 1990; Liebert et al 2003); (Kawka et al 2007). Isolated WDs can be separated into two groups - high field magnetic WDs (HFMWDs) with magnetic fields stronger than 10^6 G and the rest with lower magnetic fields typically $< 10^5$ G. About 10% of isolated WDs are HFMWDs (Liebert et al 2005; Kawka et al 2007; Tout et al 2008). Recent studies point toward a binary origin of HFMWDs (see e.g. (García-Berro et al 2012) and references therein).

Many stars are born in the binary systems going through one or more phases of the mass-exchange (Winget & Kepler 2008; Kawka & Vennes 2014); (Tremblay et al 2015; Mukai 2017). Numerous observed accreting WDs are often surrounded by an accretion gas of companion star / disk (Begelman et al 1984; Mukai 2017). Cataclismic Variables (CVs) and Symbiotics are representing the accreting white dwarf binaries (AWBs). A WD with a close companion that is overflowing its Roche lobe is a cataclismic variable (CV) (Warner 1995; Liebert et al 2005). Depending on the magnetic field, there are two classes of CVs: nonmagnetic CVs characterised by their eruptive behavior (Warner 1995; Balman 2020; Mukai 2017), with weak or nonexistent magnetic fields ($< 0.01MG$) and the magnetic CVs (MCVs), divided into two sub-classes as Polars (with strong magnetic fields in the range of (20 – 230) MG, which cause the accretion flow to directly channel onto the magnetic poles of the WD inhibiting the formation of an accretion disk) and Intermediate Polars, which have a weaker field strength of (1-20) MG, (Warner 1995; Mouchet et al 2012; Mukai 2017). Among the CVs

K. Kotorashvili

¹Department of Physics, Faculty of Exact & Natural Sciences, Javakishvili Tbilisi State University, Tbilisi 0179, Georgia

N.L. Shatashvili

¹Department of Physics, Faculty of Exact & Natural Sciences, Javakishvili Tbilisi State University, Tbilisi 0179, Georgia

²Andronikashvili Institute of Physics, TSU, Tbilisi 0177, Georgia

*E-mail: nana.shatashvili@tsu.ge

about 25% (Wickramasinghe & Ferrario 2000) have WDs that are very magnetic (Balman 2020).

It was proposed recently that WD magnetic fields have a fossil origin (Braithwaite & Spruit 2014) originally suggested for Sun (Couling 1945). An alternative suggestion is that they could be generated by a dynamo process in the star's convective core (Ferrario et al 2015) or/and during the star's evolution common envelope phase by accreting disk-dynamo (Nordhaus et al 2010). However, fossil origin idea has difficulty explaining high field strengths and the observed lack of a correlation with rotation as well as the absence of field configurations stable enough to survive in a star over its lifetime (Braithwaite & Spruit 2014).

According to (Tout et al 2008) the fact that WDs with a surface magnetic field over 3 MG has not been found in a detached binary system suggests that all such highly magnetic WDs have a binary origin, which relies on a magnetic dynamo (D) during the common envelope (CE) phase of binary evolution. If the two stars merge the end product is a single HFMD that may later evolve into the MCVs (Ferrario et al 2020).

In addition to the magnetic field it is expected, that large-scale outflows met in various astrophysical setting being the collimated long-lived structures related to accreting disks surrounding the compact objects [see e.g. (Begelman et al 1984) and references therein] are also playing an important role in stellar evolution, including late stages of their lives and their final fates. AWBs are important laboratories for accretion and outflow physics. In CVs (nova-likes) the outflow velocities can vary within 200-5000 km/s (Long et al 2002; Kafka & Honeycutt 2004; Puebla et al 2011).

For a typical cold magnetic WD with degenerate electron densities $\sim (10^{25} - 10^{29})\text{cm}^{-3}$ and magnetic fields $\sim (10^5 - 10^9)\text{G}$, temperatures are $\sim (40000 - 6000)\text{K}$ (Kawka & Vennes 2014; Hollands et al 2015). At very high densities, particle Fermi Energy can become relativistic and degeneracy pressure (μ_0) may dominate thermal pressure (β_0); for these parameters, Alfvén velocity $V_A \sim (10^4 - 10^6)\text{cm/s}$, yielding plasma $\beta_0 \sim (10^6 - 10^0)$, $\mu_0 \sim (10^{10} - 10^6)$ leading to $\mu_0 \gg \beta_0$, so the plasma may be treated as cold, even with temperature $\sim 10^9\text{K}$ (Berezhiani et al 2015).

The consequences of degeneracy in multi-component plasma were studied recently in terms of multi-scale behavior (Berezhiani et al 2015; Shatashvili et al 2016); (Barnaveli & Shatashvili 2017) to investigate effects of degeneracy e.g., on the dynamics of the star collapse that seems to be sensitive to outer layers/atmosphere composition, structure and their conditions. These studies have shown the generation/amplification of fast macro-scale plasma flows in the degenerate two-fluid

astrophysical systems, for which the simplest relaxed states are described by double Beltrami condition, which states that the generalized flow is aligned with its vorticity augmented by the Bernoulli condition.

Shatashvili et al (2019) have shown that in a quasi neutral plasma of a bulk degenerate electrons contaminated by small fraction of a non-degenerate highly relativistic hot electron component can induce a new scale (for structure formation) to a system consisting of an ion-degenerate electron plasma. Determined by concrete parameters of the system, new macro-scale lengths (much larger than short intrinsic scale lengths [skin depths] and generally much shorter than system size) open new pathways for energy transformations. It is expected that this combination of plasmas will also pertain during the relativistic jet formation from accretion-induced collapsing WDs to Black Holes (Begelman et al 1984; Krivdyk 1999; Krivdyk & Agapitov 2007).

The main goal of the paper is to find the possible mechanism for the origin and evolution of large-scale magnetic/velocity fields in multi-component compact astrophysical objects and their vicinity; more precisely we will examine the possible role played by the Unified Reverse Dynamo (RD)/Dynamo in explaining the existence of macro-scale flow and magnetic field in a highly degenerate (d) WD plasma co-existing with a classical hot (h) accreting astrophysical flow. We will investigate the role of degeneracy effects and explore the new physics originating from the contamination of the (h) component in the formation of macro-scale magnetic and velocity fields to uncover the effects of magneto-fluid couplings of accreting stars since the dynamical evolution of their convective envelopes may define the final structure of their interior as well as of atmospheres.

2 Model Equations for Unified Reverse Dynamo / Dynamo mechanism for 2-Temperature Relativistic e-i plasmas of astrophysical objects

In our recent paper (Kotorashvili et al 2020) from an analysis of the degenerate two-fluid (electron-ion or electron-positron) system, we have extracted the Unified RD/D mechanism (Mahajan et al 2005;2006; Lingam & Mahajan 2015) - the amplification / generation of fast macro-scale plasma flows in astrophysical systems with initial turbulent (micro-scale) magnetic/velocity fields. It was shown that the generated/accreted locally super-Alfvénic flows are extremely fast with Alfvén Mach number $> 10^3$ as observed in different astrophysical outflows. This process

is simultaneous with and complementary to the micro-scale unified dynamo - generation of macro-scale flows is an essential consequence of magneto-fluid coupling; generation of macro-scale fast flows and magnetic fields are simultaneous, they grow proportionately.

In this section we will be studying a quasi neutral plasma of an immobile classical ion component (i), and two relativistic electron species - the bulk d electron gas with a density N_{0d} and a small contamination of h electrons with density N_{0h} . In our simplified model the gravity (Newtonian) effects are ignored when solving the Dynamo/Reverse Dynamo problem to show the tendency of such complex system to generate large-scale Magnetic/Velocity fields locally; hence, the density variations are ignored, such effects are important at the distances where the catastrophic transformation of energy takes place (Mahajan et al 2002; Barnaveli & Shatashvili 2017); and the wave-coupling phenomena (see e.g. (Shatashvili et al 2020)) are beyond the scope of present study; note, that for a disk-jet structure formation both the gravity and rotation effects were studied in (Shatashvili & Yoshida 2011; Arshilava et al. 2019). This model can be applied for the description of the system of dense/degenerate WD's outer layer that accretes a classical hot astrophysical flow. Also, based on the observations, we assumed that hot electron fluid fraction is small and in such three component plasma ion fluid velocities are much smaller than those for lighter electron (d, h) fluids [$\mathbf{V}_i \ll \mathbf{V}_d, \mathbf{V}_h$]. Thus, ion dynamics is neglected (Oliveira & Tajima 1995). Then, following Shatashvili et al. (2019) we write for quasi neutrality condition

$$N_{0d} + N_{0h} = N_{0i} \implies \frac{N_{0i}}{N_{0d}} = 1 + \alpha, \quad \alpha \equiv \frac{N_{0h}}{N_{0d}}, \quad (1)$$

where $\alpha \ll 1$ labels the ratio of hot electron fraction to the degenerate electrons. Notice, that flow effects were found crucial in creating the structural richness, in the heating/cooling processes, in Generalized Dynamo theory and outflow formation in astrophysical environments (Mahajan et al 2001; Mahajan et al 2002; Mahajan et al 2005;2006; Lingam & Mahajan 2015); (Kotorashvili et al 2020) and since in our system there are two symmetry-breaking mechanisms: 1) one is due to different effective inertias for the d and h electrons, and 2) the other is from the small h contamination added to the bulk d electrons ($\alpha \neq 0, \mathbf{V}_h \neq 0$), both of them are responsible for creating a net "current". The structure formation mechanism originates, for instance, in the effective inertia difference (see e.g. (Berezhiani & Mahajan 1994,1995; Berezhiani et al 2010) and references therein). Asymmetry between the plasma constituents increases the

number of conserved helicities, and eventually translates into a higher index equilibrium Beltrami state (Mahajan & Lingam 2015; Shatashvili et al 2016); (Shatashvili et al 2019) and creation of electron-sound (Shatashvili et al 2020) in such complex relativistic environment. We will show below that even in the case of immobile ions when the rotation effects are ignored (important for pulsars/pulsar binaries (Krishnan et al 2020) and not the case of present study) these asymmetries strongly define the dynamics of Unified Dynamo/Reverse dynamo action and lead to very interesting and new scenarios for fast super-Alfénic flow/outflow formation or/and strong magnetic field formation in the vicinity of WDs that accrete hot astrophysical flow.

We remind the reader that the effective mass factor $G_d(n_d) = \sqrt{1 + \left(\frac{n_d}{n_c}\right)^{\frac{2}{3}}}$ for degenerate electron plasma originates from degeneracy rather than kinematics and is fully determined by the plasma rest frame density $n_d = N_d/\gamma_d$ (see (Berezhiani et al 2015) and references therein) for arbitrary n_d/n_c (with $n_c = 5.9 \cdot 10^{29} \text{ cm}^{-3}$ being the critical number-density). While for relativistically hot electron plasma the effective mass factor $G_h = \frac{5}{2} \frac{T_e}{m_e c^2} + \frac{3}{2} \sqrt{\left(\frac{T_e}{m_e c^2}\right)^2 + \frac{4}{9}}$ (Mignone et al 2005; Ryu et al 2006) is determined by the relativistic electron temperature T_e . As mentioned above below we consider the analytically tractable constant-density system to study the Unified Dynamo/RD phenomena in our complex 2-temperature relativistic system, assuming quasi-neutrality $\varphi \equiv 0$, and for simplicity we put $\gamma_d \sim \gamma_h \sim 1$ leading to $G_d = \text{const} \equiv G_0(n_{0d})$, $G_h = \text{const} \equiv H_0(T_{e0})$ (Shatashvili et al 2019).

The electron dynamics for both components can be described by the appropriate relativistic fluid equations (see e.g. (Berezhiani et al 2015) and references therein): the continuity and the equation of motion (Shatashvili et al 2019) that can be cast into an ideal vortex dynamics in terms of the generalized (canonical) vorticities. Our model pertains only for homentropic plasmas; for special astrophysical conditions, canonical vorticity would have a quantum-mechanical part [see (Mahajan & Asenjo 2011; Asenjo & Mahajan 2015) for spinning plasmas], and even a general relativistic component [see e.g. (Bhattacharjee et al 2015) for Black Hole accretion disks] in addition to the electromagnetic, kinetic and thermal contributions; for most applications these corrections are negligibly small. Moreover, even for the highly relativistic case when the space-time metric is almost Minkowskian and terms of order $O(c^{-4})$ or higher are neglected, it is possible to write the (linearized) equations of general relativity (GR) in a form that is almost identical to that of the Maxwell equations

of ordinary electromagnetism (see e.g. (Manfredi 2014) and references therein). Then, in the dimensionless form these equations for 2-temperature relativistic plasma consisted of bulk degenerate e-i plasma contaminated by relativistically hot electron ion plasma in the limit of immobile ions can be reduced to (where \mathbf{b} and $\mathbf{V}_{d(h)}$ are the dimensionless magnetic and velocity fields, respectively):

$$\begin{aligned}
& \left(G_0 + \frac{H_0}{\alpha} \right) \frac{\partial \mathbf{b}}{\partial t} + G_0 \frac{H_0}{\alpha} \frac{\partial}{\partial t} \nabla \times \nabla \times \mathbf{b} = \\
& = \frac{(H_0 - G_0)}{\alpha} \nabla \times \mathbf{V}_d \times \mathbf{b} + \frac{G_0}{\alpha} \nabla \times (\mathbf{b} \times (\nabla \times \mathbf{b}) - \\
& - \frac{G_0 H_0}{\alpha^2} \nabla \times (\mathbf{V}_d \times \nabla \times \mathbf{V}_d + \mathbf{V}_d \times \nabla \times \nabla \times \mathbf{b}) - \\
& - \frac{G_0 H_0}{\alpha^2} \nabla \times ((\nabla \times \mathbf{b}) \times \nabla \times \mathbf{V}_d) - \\
& - \frac{G_0 H_0}{\alpha^2} \nabla \times ((\nabla \times \mathbf{b}) \times \nabla \times (\nabla \times \mathbf{b})) , \quad (2) \\
& \left(G_0 + \frac{H_0}{\alpha} \right) \frac{\partial \mathbf{V}_d}{\partial t} + \frac{H_0}{\alpha} \frac{\partial}{\partial t} \nabla \times \mathbf{b} = - \frac{1}{\alpha} \mathbf{V}_d \times \mathbf{b} + \\
& + \frac{1}{\alpha} \mathbf{b} \times (\nabla \times \mathbf{b}) - \left(\frac{H_0}{\alpha^2} - G_0 \right) \mathbf{V}_d \times \nabla \times \mathbf{V}_d - \\
& - \frac{H_0}{\alpha^2} \mathbf{V}_d \times \nabla \times (\nabla \times \mathbf{b}) + \\
& + \frac{H_0}{\alpha^2} ((\nabla \times \mathbf{b}) \times \nabla \times \mathbf{V}_d + (\nabla \times \mathbf{b}) \times \nabla \times \nabla \times \mathbf{b}) ,
\end{aligned}$$

that can be closed by Ampere's law

$$\nabla \times \mathbf{b} = - \mathbf{V}_d - \alpha \mathbf{V}_h , \quad (4)$$

where density is normalized to N_{0d} (corresponding rest-frame density is n_{0d}); the magnetic field is normalized to some ambient measure $|\mathbf{B}_0|$; hot electron gas temperature is normalized to $m_e c^2$; all velocities are measured in terms of the corresponding Alfvén speed $V_A = V_{Ad} = B_0 / \sqrt{4\pi n_{0d} m_e G_{0d}}$ all lengths [times] are normalized to the "effective" degenerate electron skin depth $\lambda_{\text{eff}}^d [\lambda_{\text{eff}}^d / V_A]$ with $\lambda_{\text{eff}}^d = c / \omega_{pe}^d = c \sqrt{m_e G_{0d} / 4\pi n_{0d} e^2}$.

Following the standard procedure Mahajan et al. (2005) let's assume that our total fields are composed of some ambient seed fields and fluctuations about them taking into account relativistic effects both for bulk degenerate electron-fluid and hot electron fraction:

$$\mathbf{b} = \mathbf{b}_0 + \tilde{\mathbf{b}}, \quad \mathbf{V}_{d(h)} = \mathbf{v}_{0d(oh)} + \mathbf{U}_{d(h)} + \tilde{\mathbf{v}}_{d(h)} , \quad (5)$$

where \mathbf{b}_0 and $\mathbf{v}_{0d(oh)}$ are the equilibrium fields, \mathbf{B} , $\mathbf{U}_{d(h)}$ are the macroscopic fluctuations and $\tilde{\mathbf{b}}$, $\tilde{\mathbf{v}}_{d(h)}$ are the microscopic fluctuations, respectively. We remind that the energy reservoir comes from the background fields, which have both macroscopic and microscopic components feeding the macro- and micro-scale fluctuations of fields. To describe background fields, for analytical work, we choose a special class of equilibrium Beltrami-Bernoulli (BB) solutions to the equations (2) and (3) (see e.g. (Mahajan et al 2005;2006; Lingam & Mahajan 2015; Kotorashvili et al 2020)) for both degenerate d and hot h electrons well studied in (Shatashvili et al 2019) that reduce to:

$$\mathbf{b}_0 - G_0 \nabla \times \mathbf{v}_{0d} = a_d \mathbf{v}_{0d}, \quad \mathbf{b}_0 - \mathbf{H}_0 \nabla \times \mathbf{v}_{0h} = \alpha a_h \mathbf{v}_{0h} \quad (6)$$

which, following the straightforward algebra, reduces to a Triple Beltrami (TB) equation for \mathbf{b}_0 :

$$\begin{aligned}
& G_0 \frac{H_0}{\alpha} \nabla \times \nabla \times \nabla \times \mathbf{b}_0 + \left(a_d \frac{H_0}{\alpha} + a_h G_0 \right) \nabla \times \nabla \times \mathbf{b}_0 \\
& + \left(G_0 + \frac{H_0}{\alpha} + a_d a_h \right) \nabla \times \mathbf{b}_0 + \left(a_d + a_h \right) \mathbf{b}_0 = 0, \quad (7)
\end{aligned}$$

and relations for \mathbf{v}_{0d} and \mathbf{v}_{0h} ($\eta \equiv a_d \frac{H_0}{\alpha} - a_h G_0$):

$$\begin{aligned}
\mathbf{v}_{0d} & = \eta^{-1} \left(G_0 \frac{H_0}{\alpha} \nabla \times \nabla \times \nabla \times \mathbf{b}_0 \right) + \\
& + \eta^{-1} \left[a_h G_0 \nabla \times \mathbf{b}_0 + \left(G_0 + \frac{H_0}{\alpha} \right) \mathbf{b}_0 \right] , \quad (8) \\
\mathbf{v}_{0h} & = - \frac{\eta^{-1}}{\alpha} \left(G_0 \frac{H_0}{\alpha} \nabla \times \nabla \times \nabla \times \mathbf{b}_0 \right) - \\
& - \frac{\eta^{-1}}{\alpha} \left[a_d \frac{H_0}{\alpha} \nabla \times \mathbf{b}_0 + \left(G_0 + \frac{H_0}{\alpha} \right) \mathbf{b}_0 \right] , \quad (9)
\end{aligned}$$

where $\nabla \cdot \mathbf{b}_0 = 0$, $\nabla \cdot \mathbf{v}_{0d(oh)} = 0$ are automatically satisfied and $a_{d(h)}$ are dimensionless constants related to two invariants: $h_{d(h)} = \int d^3x (\mathbf{A} \pm G_0(H_0) \mathbf{v}_{0d(oh)}) \cdot (\mathbf{b}_0 \pm G_0(H_0) \nabla \times \mathbf{v}_{0d(oh)})$ - the generalized helicities of $d(h)$ relativistic electron fluids. Here the generalized vorticities for both fluids have now both magnetic and kinetic parts due to the corresponding relativistic effects. We need to choose these constants (that together with the defining parameters G_0, H_0, α fully determine the equilibrium system) so that the scales [solutions of the equation $G_0 \frac{H_0}{\alpha} \mu^3 + (a_d \frac{H_0}{\alpha} + a_h G_0) \mu^2 + (G_0 + \frac{H_0}{\alpha} + a_d a_h) \mu + (a_d + a_h) = 0$] are vastly separated. Following the similar procedure as in (Mahajan et al 2005;2006; Lingam & Mahajan 2015; Kotorashvili et al 2020), assuming that main energy reservoir is in micro-scale equilibrium component and $|\tilde{\mathbf{b}}| \ll |\mathbf{b}_0|$, $|\tilde{\mathbf{v}}_{d(h)}| \ll$

$|\mathbf{v}_{0d(\mathbf{oh})}|$ we find that the equilibrium velocity and magnetic fields are related as

$$\mathbf{v}_{0d(h)} = \chi_{d(h)} \mathbf{b}_0, \quad (10)$$

where χ_d and χ_h are given by

$$\chi_d \equiv \eta^{-1} \left[G_0 \frac{H_0}{\alpha} \lambda^2 + a_h G_0 \lambda + \left(G_0 + \frac{H_0}{\alpha} \right) \right],$$

$$\chi_h \equiv -\frac{\eta^{-1}}{\alpha} \left[G_0 \frac{H_0}{\alpha} \lambda^2 + a_d \frac{H_0}{\alpha} \lambda + \left(G_0 + \frac{H_0}{\alpha} \right) \right]. \quad (11)$$

The straightforward algebra gives the following equations for micro-scale magnetic and degenerate fluid velocity fields (the derivations for relativistically hot fluid component relations see the Appendix-A):

$$m \frac{\partial \tilde{\mathbf{b}}}{\partial t} + m_1 \frac{\partial}{\partial t} \nabla \times \nabla \times \tilde{\mathbf{b}} = (\mathbf{Q}_d \cdot \nabla) \mathbf{b}_0, \quad (12)$$

$$m \frac{\partial \tilde{\mathbf{v}}_d}{\partial t} + q_1 \frac{\partial}{\partial t} \nabla \times \tilde{\mathbf{b}} = (\mathbf{S}_d \cdot \nabla) \mathbf{b}_0, \quad (13)$$

where \mathbf{Q}_d and \mathbf{S}_d are functions of \mathbf{U}_d and \mathbf{B} , as well as plasma-system parameters. Using (12), (13) we obtain the final equations for macro-scale \mathbf{B} and \mathbf{U}_d :

$$m_1 \nabla \times \nabla \times \ddot{\mathbf{B}} + m \ddot{\mathbf{B}} = r_d \nabla \times \mathbf{B} + p_d \nabla \times \mathbf{U}_d. \quad (14)$$

$$q_1 \nabla \times \ddot{\mathbf{B}} + m \ddot{\mathbf{U}}_d = q_d \nabla \times \mathbf{B} + s_d \nabla \times \mathbf{U}_d, \quad (15)$$

where

$$m_1 = \frac{G_0 H_0}{\alpha} \left(G_0 + \frac{H_0}{\alpha} \right), \quad m = \left(G_0 + \frac{H_0}{\alpha} \right)^2,$$

$$q_1 = \frac{H_0}{\alpha} \left(G_0 + \frac{H_0}{\alpha} \right), \quad (16)$$

and the constants

$$r_d = \frac{\lambda b_0^2}{3} \left[\frac{H_0 - G_0}{\alpha^2} - \frac{G_0 H_0}{\alpha^3} \lambda (\chi_d + \lambda) + \left(\frac{G_0}{\alpha} (\chi_d + \lambda) - \frac{H_0}{\alpha} \chi_d \right)^2 \right],$$

$$p_d = -\frac{\lambda b_0^2}{3} \left[\frac{H_0 - G_0}{\alpha} - \frac{G_0 H_0}{\alpha^2} \lambda (\chi_d + \lambda) \right] \left(\frac{H_0 - G_0}{\alpha^2 \lambda} - \frac{G_0 H_0}{\alpha^3} (\chi_d + \lambda) + \frac{H_0}{\alpha^2} (\chi_d + \lambda) - \chi_d G_0 - \right.$$

$$\left. - \frac{G_0}{\alpha} (\chi_d + \lambda) - \frac{H_0}{\alpha} \chi_d \right),$$

$$q_d = -\frac{\lambda b_0^2}{6} \left[\left(\frac{G_0}{\alpha} (\chi_d + \lambda) - \frac{H_0}{\alpha} \chi_d \right) \cdot \left(\frac{H_0^2}{\alpha^2 q_1} \chi_d \lambda (G_0 + 1) + \frac{G_0 H_0}{\alpha^2 q_1} + \frac{H_0}{\alpha^2} \lambda (\chi_d + \lambda) \right) - \frac{H_0}{\alpha^3} (\chi_d + \lambda) + \frac{G_0}{\alpha} \chi_d \right],$$

$$s_d = -\frac{\lambda b_0^2}{6} \left[\left(\frac{H_0}{\alpha^3 \lambda} (\chi_d + \lambda) - \frac{G_0}{\alpha \lambda} \chi_d + \frac{H_0}{\alpha^2} (\chi_d + \lambda) - \chi_d G_0 \right) + \left(\frac{(H_0 - G_0)}{\alpha} - \frac{G_0 H_0}{\alpha^2} \lambda (\chi_d + \lambda) \right) \cdot \left(\frac{H_0^2}{\alpha^2 q_1} \chi_d \lambda (G_0 + 1) + \frac{G_0 H_0}{\alpha^2 q_1} + \frac{H_0}{\alpha^2} \lambda (\chi_d + \lambda) \right) \right], \quad (17)$$

where $b_0^2 (v_0^2)$ measures the ambient micro-scale (turbulent) magnetic (kinetic) energy and all the coefficients are functions of background system defining parameters $G_0, H_0, \alpha, \lambda, a_d, a_h$ (hence, determined by energies, effective masses, fraction coefficient and helicities).

Performing a Fourier analysis we obtain the following dispersion relation (DR):

$$\omega_d^8 m'^2 m^2 - \omega_d^4 k^2 \left(2m' m p_d q'_d + m^2 r_d^2 + m'^2 s_d^2 \right) + (p_d q'_d - r_d s_d)^2 k^4 = 0, \quad (18)$$

$$\text{with} \quad m' = (m + m_1 k^2), \quad q'_d = (q_d + q_1 \omega^2)$$

and, finally, using the same procedure for hot relativistic fluid (presented in Appendix-A) we derive the relations for all macro-scale fluctuations of vector-fields (with corresponding DRs (18) and (A5)):

$$\mathbf{U}_{d(h)} = \frac{q'_{d(h)} \left[\omega_{d(h)}^4 m' m - (p_{d(h)} q'_{d(h)} - r_{d(h)} s_{d(h)}) k^2 \right]}{\omega_{d(h)}^4 m^2 r_{d(h)} + s_{d(h)} [p_{d(h)} q'_{d(h)} - r_{d(h)} s_{d(h)}] k^2} \mathbf{B}, \quad (19)$$

Equations (19) are the manifestation of Unified Dynamo/Reverse Dynamo - a simultaneous generation of large-scale magnetic field and flow from ambient short-scale turbulent energy (magnetic or/and kinetic) - a manifestation of magneto-fluid coupling. Interestingly, relations between fields have the same form for degenerate and hot fluids but we shall remember, that

defining coefficients $[r_{d(h)}, p_{d(h)}, q_{d(h)}, s_{d(h)}]$ are different for these fluids as well as the solutions of corresponding dispersion relations are different. Thus, the larger the ambient system turbulent energy is, the stronger the flow acceleration will be; for more details the reader may consult with (Mahajan et al 2005;2006; Lingam & Mahajan 2015; Kotorashvili et al 2020)).

We also observe that to leading order, due to hot relativistic fluid contamination, evolution of \mathbf{B} does require knowledge of \mathbf{U}_d and vice versa (compare with degenerate e-i case (Kotorashvili et al 2020), when knowledge of \mathbf{B} does not require knowledge of \mathbf{U}_d); note, that now similar conclusion is valid for \mathbf{U}_h ; hence, magneto-fluid coupling process is much richer now leading to various scenarios for magnetic field generation or/and flow acceleration both for degenerate and hot components. In the next section we will show how the choice of system parameters define final fate of the system. From various scenarios we chose 2 limiting simplest cases for illustration (interesting for WDs accreting hot astrophysical flow):

- (i) $a_d = -a_h \equiv a$ and Beltrami index goes from triple to double. For WDs with $n_0 \equiv 10^{25} - 10^{29} \text{ cm}^{-3}$ leading to $G_0 \geq 1.5$ and for $H_0 > 1$, $\alpha \ll 1$ we have $\frac{H_0}{\alpha} \gg G_0$. When choosing the inverse micro-scale to be $\lambda = -\frac{\alpha}{2G_0H_0} \left[a \left(\frac{H_0}{\alpha} - G_0 \right) + \left(\frac{H_0}{\alpha} + G_0 \right) \sqrt{a^2 - \frac{4G_0H_0}{H_0 + \alpha G_0}} \right]$ we find that for $a > G_0 + 1$ the ambient energy is mostly kinetic while for $2\sqrt{G_0} < a < G_0 + 1$ the ambient energy is mostly magnetic.
- (ii) $a_d = \frac{1}{a_h}$, for which numerically solving the the relevant equation to find scales we could find the regimes to determine the dominance of magnetic/kinetic energies in the ambient energy of the system.

Notice, that for small \mathbf{k} we have $m' \simeq m$, $q'_{d(h)} \simeq q_{d(h)}$ and from dispersion relations (18) and (A5) we obtain for degenerate and hot fluids, respectively:

$$\omega_{d(h)}^4 = \frac{k^2}{2m} \left[2p_{d(h)}q_{d(h)} + r_{d(h)}^2 + s_{d(h)}^2 \pm (r_{d(h)} + s_{d(h)}) \sqrt{(r_{d(h)} - s_{d(h)})^2 + 4p_{d(h)}q_{d(h)}} \right] \quad (20)$$

and, consequently, the relations between fields read as:

$$\mathbf{U}_{d(h)} = \left[\frac{s_{d(h)} - r_{d(h)}}{2p_{d(h)}} \pm \frac{1}{2p_{d(h)}} \sqrt{4p_{d(h)}q_{d(h)} + (r_{d(h)} - s_{d(h)})^2} \right] \mathbf{B}. \quad (21)$$

Thus, we see, that besides the ambient system-defining parameters, the relations between macro-fields are strongly dependent also on corresponding DR solution and range of \mathbf{k} . Below we show how the Unified RD/D related phenomena influence the evolution

dynamics of 2-Temperature relativistic e-i plasmas of astrophysical objects.

3 Unified Dynamo/Reverse Dynamo for 2-Temperature Relativistic e-i plasmas of astrophysical objects

We performed the extensive numerical analysis study of the derived equations. For an illustrative analysis we choose the characteristic case of WD with degenerate effective mass $G_0 = 1.5$ (corresponding electron number density $\sim 10^{30} \text{ cm}^{-3}$). For an accreting hot contamination we present results for two cases of $H_0 = 1.5$ and $H_0 = 10$ (corresponding electron temperatures $2.2 \cdot 10^9 \text{ K}$ and $1.5 \cdot 10^{10} \text{ K}$, respectively). As an example we considered two extreme cases of following DB parameters: (i) $a_d = -a_h \equiv a$ and (ii) $a_d = \frac{1}{a_h} \equiv a$; for all cases $\alpha = 0.001$ since the detailed analysis showed no significant dependence on α as long as it is ≤ 0.01 .

(i) For the case $a_d = -a_h \equiv a$ we have explored various interesting cases among which we present below 2 simplest examples for $k \rightarrow 0$ and characteristic limits for Beltrami parameter a so that for dispersion relations we use equations (20) for degenerate (hot) fluids:

(i-1) For the range of $2.5 < a < 15$ we have $\mathbf{v}_{0h} \ll \mathbf{b}_0 \ll \mathbf{v}_{0d}$ meaning that the ambient degenerate flow is primarily kinetic while the ambient hot one is magnetically dominant; the plots display the results for 2 different hot fluid temperatures: $H_0 = 1.5$ (red and magenta) and $H_0 = 10$ (blue and green). In Fig.1 the Alfvén Mach numbers for both fluids generated macro- and micro-scale fields are displayed for the solutions of $\omega_{d1}^4 = \frac{k^2}{2m} \left(2p_d q_d + r_d^2 + s_d^2 + (r_d + s_d) \sqrt{(r_d - s_d)^2 + 4p_d q_d} \right)$ (left column) and $\omega_{h1}^4 = \frac{k^2}{2m} \left(2p_h q_h + r_h^2 + s_h^2 + m(r_h + s_h) \sqrt{(r_h - s_h)^2 + 4p_h q_h} \right)$ (right column), while the results for the solutions of $\omega_{d2}^4 = \frac{k^2}{2m} \left(2p_d q_d + r_d^2 + s_d^2 - (r_d + s_d) \sqrt{(r_d - s_d)^2 + 4p_d q_d} \right)$ (left column) and $\omega_{h2}^4 = \frac{k^2}{2m} \left(2p_h q_h + r_h^2 + s_h^2 - m(r_h + s_h) \sqrt{(r_h - s_h)^2 + 4p_h q_h} \right)$ (right column) are displayed in Fig.2. We observe, that dynamics is quite different for these 2 cases - in the former case we get for both-scale fields the Reverse Dynamo scenario with Super-Alfvénic generated fields; specifically hot fluid fluctuations are very fast (Mach numbers are within $(1 - 10)$ for degenerate flow and $(1 - 5) \cdot 10^2$ for hot flow); for the latter case the scenario is the one of Dynamo: degenerate fluid macro- as well as micro-scale and hot fluid velocity fluctuations are no more strong - we could call this scenario the Unified Reverse Dynamo/Dynamo process for hot fraction when

the large scale hot-flow is Super-Alfvénic and the short-scale one is sub-Alfvénic. The results are practically independent of H_0 except for micro-scale hot fluid components (that decrease with increasing a). The entire process is the illustration of Unified Dynamo/Reverse Dynamo process for a mixed system predicting the generation of strong magnetic fields of both scales simultaneously to the weak flows/outflows in the 2-temperature relativistic complex system. This may explain the existence of strong magnetic fields in the vicinity of accreting massive stars (see e.g. (Braithwaite & Spruit 2014; Tutukov & Cherepashchuk 2020) & references therein).

(i-2). For the range of $2.45 \leq a < 2.5$ we have $\mathbf{b}_0 \gg \mathbf{v}_{0d}, \mathbf{v}_{0h}$ meaning that both degenerate fluid and relativistically hot fluid-contamination are primarily magnetic; the plots display the results for $H_0 = 1.5$ (red and magenta) and $H_0 = 10$ (blue and green). In Fig.3 the Alfvén Mach numbers for both fluids generated macro- and micro-scale fields are displayed for the solutions ω_{d1}^4 (left column) and ω_{h1}^4 (right column), while the results for the solutions ω_{d2}^4 (left column) and ω_{h2}^4 (right column) are displayed in Fig.4. We again observe, that the dynamics is quite different for these 2 cases - for the former case the generated degenerate flows are practically Alfvénic in both scales while the hot flows are super-Alfvénic (with Mach numbers within $(1 - 5) \cdot 10^2$ - straight Reverse Dynamo scenario, independent of ambient temperature) and for the latter case we have purely Dynamo process in both fluids and both-scales - such scenario can explain the generation of strong magnetic fields in the envelope phase of star accretion, for instance cases of intermediate-field WDs found in CVs and some HFMWDs are argued to be formed through interface dynamo / disk dynamo processes (Tout et al 2008; Nordhaus et al 2010). We remind the reader, that such combined scenario is absent in pure degenerate e-i case for the primarily magnetic ambient system, hence, such possibility is entirely due to the hot contamination found in accreting stars / binary system; the unified Dynamo/RD scenario was found for degenerate e-i system only for kinetic ambient system argued to explain the core-dynamo (Ruderman & Sutherland 1973; Kissin & Thommpson 2015) formation of magnetic fields of HFMWDs (Kotorashvili et al 2020). Interestingly, existence of Super-Alfvénic large-scale hot-flows for our composite system (with different solutions of dispersion relations co-existing in both fluids) may explain the formation of transient jets fed by short-scale fluctuations of both fluids that follow Dynamo - a well established path of Unified Dynamo/Reverse Dynamo.

We have examined the dependence of final results on the hot relativistic fraction ambient temperature H_0 .

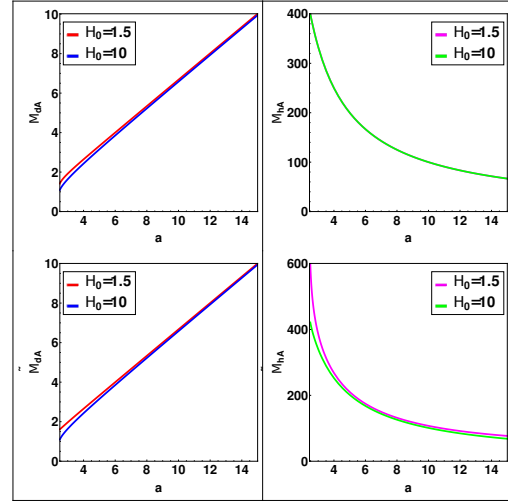


Fig. 1 Plots for Alfvén Mach numbers versus Beltrami parameter $a_d = -a_h \equiv a$ (case (i-1)) for degenerate fluid (left column) for the ω_{d1} solutions and for hot relativistic fluid (right column) for the solutions of ω_{h1} . Reverse Dynamo for both fluids in both the macro- and micro-scale components - hot flow is strongly Super-Alfvénic. Plots display the results for 2 different hot fluid temperatures: $H_0 = 1.5$ (red and magenta) and $H_0 = 10$ (blue and green). The results are practically independent of H_0 except for micro-scale hot component Mach numbers that decrease with increasing a .

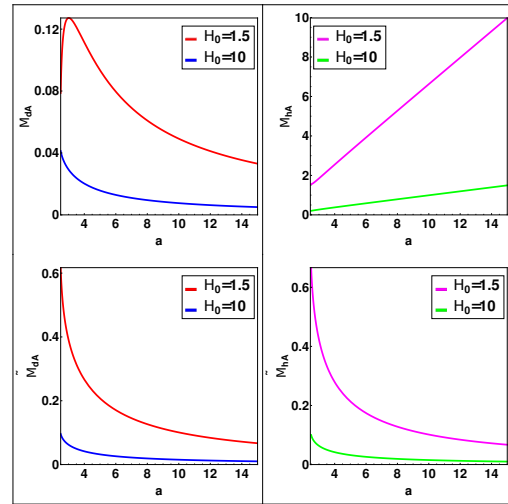


Fig. 2 Plots for Alfvén Mach numbers versus Beltrami parameter $a_d = -a_h \equiv a$ (case (i-1)) for degenerate fluid (left column) for the ω_{d2} solutions and for hot relativistic fluid (right column) for the solutions of ω_{h2} - Dynamo for degenerate and Unified D/RD for hot - Unified D/RD for entire mixed system. Plots display the results for 2 different hot fluid temperatures: $H_0 = 1.5$ (red and magenta) and $H_0 = 10$ (blue and green) that are in the same range for each component.

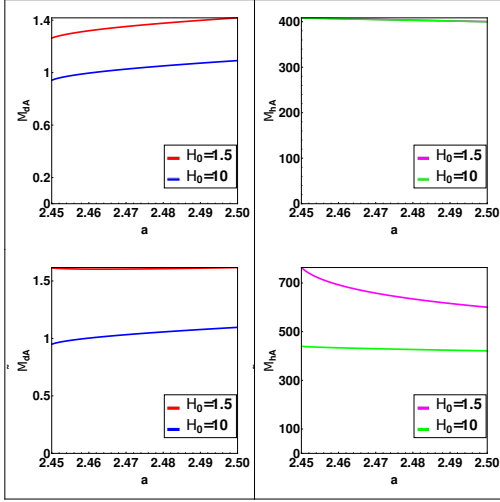


Fig. 3 Plots for Alfvén Mach numbers versus Beltrami parameter $a_d = -a_h \equiv a$ (entire ambient system is magnetically dominant - case (i-2)) for degenerate fluid (left column) for the ω_{d1} solutions and for hot relativistic fluid (right column) for the solutions of ω_{h1} . Reverse Dynamo for a mixed system - degenerate flow becomes practically Alfvénic while hot flow is strongly Super-Alfvénic in both scales. The results for macro-scale generated hot outflow coincide for different ambient temperatures.

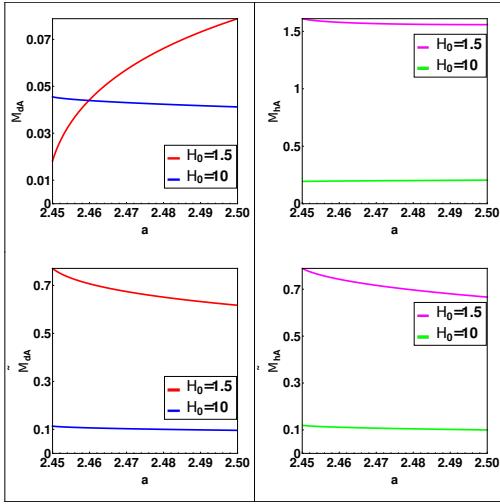


Fig. 4 Plots for Alfvén Mach numbers versus Beltrami parameter $a_d = -a_h \equiv a$ (entire ambient system is magnetically dominant - case (i-2)) for degenerate fluid (left column) for the ω_{d2} solutions and for hot relativistic fluid (right column) for the solutions of ω_{h2} - straight Dynamo for both fluids practically in both scales (hot fluid large-scale component is nearly Alfvénic).

As shown above for Reverse Dynamo scenarios (Figures 1,3) the Mach numbers are practically independent of H_0 . In Fig.5 we present the maximal values of Mach numbers for the 2nd roots of cases (i-1) (Fig.2) and (i-2) (Fig.4); Beltrami parameter was chosen to be $a = 10$ (blue, green - magnetically dominant degenerate fluid) for the former case and $a = 2.5$ (cyan, orange - magnetically dominant entire ambient system) for the latter. The Maximal values decrease with the increase of ambient temperature. Main result is the same for the 2nd root: there is a possibility of strong magnetic field generation while the WD envelope phase evolution when accreting the hot astrophysical flow.

(ii) For case $a_d = 1/a_h \equiv a$ we have explored various interesting cases among which we present below 2 simplest important examples for $k \neq 0$ and characteristic limits for Beltrami parameter a so that for DRs we use general equations (18) for degenerate and (A5) for hot flows, respectively; we solved them numerically and found corresponding inverse micro-scales for all scenarios. 2 characteristic examples of such solutions are displayed in Fig.6 and Fig.8 for specific ambient system conditions, different colors correspond to 4 real roots. Extensive study for different parameters showed that dispersion picture does not change much - we have always four real roots with similar \mathbf{k} -dependence.

(ii-1) For $a \sim 10$ - ambient energy is kinetically dominant only for degenerate flows ($\mathbf{v}_{0h} \ll \mathbf{b}_0 \ll \mathbf{v}_{0d}$). In Fig.7 Alfvén Mach numbers are plotted for roots 1 of Fig.6, where we observe generation of Super-Alfvénic velocity fields of hot flow for two different temperatures $H_0 = 1.5$ and $H_0 = 10$; for roots 8 of dispersion relations (not displayed here since more representative result for roots 8 is displayed in Fig. 9 for (i-2) case) of the same Fig.6 we found that much stronger Super-Alfvénic macro- and micro-scale hot flows ($> 10^6$) are generated for both temperature electrons. This is a perfect scenario for Unified Reverse Dynamo/Dynamo phenomenon both in macro- and micro-scales since the large-scale magnetic fields are generated simultaneously due to magneto-fluid coupling. Notice, that for all roots of DR the generated hot flows are stronger (2 orders stronger) than degenerate flows (in both scales).

(ii-2) For $a \sim 2.45$ - whole ambient energy is mostly magnetic ($\mathbf{b}_0 \gg \mathbf{v}_{0d}, \mathbf{v}_{0h}$). In Fig.9 Alfvén Mach numbers are plotted for roots 8 of Fig.8, where we observe generation of very strong Super-Alfvénic velocity fields of hot flow for two different temperatures $H_0 = 1.5$ and $H_0 = 10$ - both macro- and micro-scale fast hot flows ($\gtrsim 10^8$) are generated for both temperatures. We also observe, that again we have very fast flows for roots 8 while for roots 1 (not displayed here), interestingly, numerical analysis for the illustration of the qualitative study show, that M_A is practically independent of

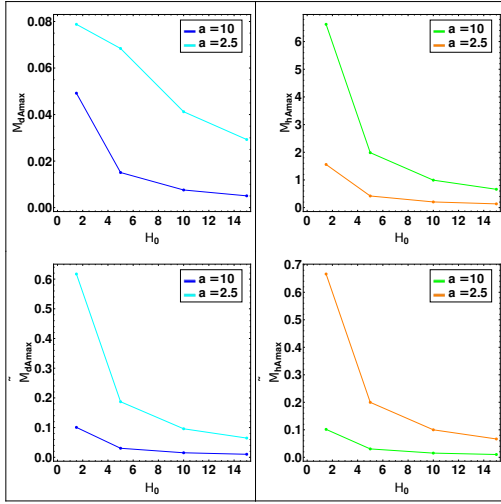


Fig. 5 Maximal values of Alfvén Mach numbers versus relativistic hot fraction ambient temperature H_0 for the cases plotted in: Fig.2 (cyan and blue) and Fig.4 (orange and green) for $a_d = -a_h \equiv a$; results are displayed for 2 limiting ambient system cases: $a = 2.5$ (cyan, orange - magnetically dominant entire system) and $a = 10$ (blue, green - magnetically dominant degenerate fluid) for degenerate fluid (left column) and for hot relativistic fluid (right column) - the bigger the H_0 the smaller is the maximal value for all scales in both fluids.

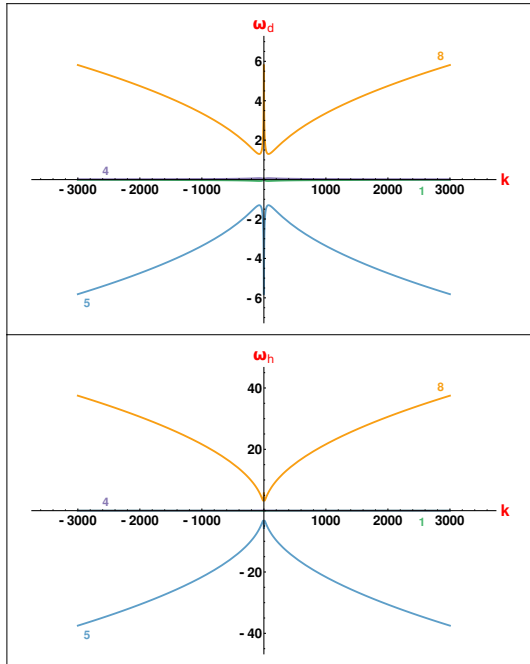


Fig. 6 Solution of dispersion relations (18) (degenerate electron flow - top) and (A5) (hot electron flow - bottom) for case (ii-1): $a_d = \frac{1}{a_h} \equiv a = 10$ - bulk ambient degenerate (hot fraction) system is kinetically (magnetically) dominant; $G_0 = 1.5$, $H_0 = 10$ (picture is similar for $H_0 = 1.5$); 4 real roots at $q \simeq q$ are displayed by different color.

k (like for case displayed in Fig.7 of (i-1) parameter range). These results could be easily explained by the dispersion relation displayed in Fig.8 - we see that for roots 1 (green) there is no significant change for big k -s, but for roots 8 (yellow) picture is very different.

We have examined the dependence of final results on the ambient relativistic hot electron fluid fraction temperature H_0 . Results for roots 8 are presented in Fig.10 showing that maximal macro-scale Alfvén Mach number M_{Amax} increases when decreasing H_0 and can reach the values $\sim 10^8$ for degenerate electron fluid ($\sim 10^{10}$ for hot electron fraction) for $H_0 = 1.5$ at $k \lesssim 10^4$. This is a perfect manifestation of Unified Reverse Dynamo / Dynamo scenario in both scales of both fluids.

Thus, analysis showed that the simultaneous dynamical generation of strong macro-scale magnetic field and fast flows/outflow is guaranteed in 2-temperature relativistic system consisting of degenerate e-i fluid and relativistically hot fluid contamination due to magneto-fluid coupling. Depending on the range of Beltrami scales (helicities) of degenerate and hot fluids (a_d and a_h) as well as density degeneracy level for former (G_0) and the temperature of latter (H_0) the ratio between macro-scale velocity and magnetic fields may become different for each fluid and for such a mixed system evolution scenarios maybe of any character; similar conclusions can be drawn for micro-scale fields. There are various scenarios for WD evolution for any type mixture of ambient bulk fluid and contamination; e.g. for specific parameter ranges two possibilities are: 1) Unified D/RD for one of the roots of DRs resulting in generation of strong magnetic fields while accretion and star formation in binary systems (García-Berro et al 2012; Briggs et al 2015). 2) Unified RD/D for some other roots of DRs resulting in generation of fast (with Mach numbers $> 10^6$) flows/outflows (Beskin 2010; Ji et al 2013); M_{Amax} is higher for $a_d = (1/a_h)$ than for $a_d = -a_h$. At the end, there can be any mixture of macro- and micro- fields in both fluids over the time but as long as the ambient hot flow fraction is magnetically dominant independently from degeneracy level and energetic character of bulk degenerate ambient fluid a formation of super-fast hot outflows (with $M_{hAmax} > 10^8 > M_{dAmax}$) is guaranteed while WD evolution. Fraction parameter $\alpha \ll 1$ value doesn't play significant role. Note, that for the global dynamics of multi-component and multi-scale plasmas accreting into WDs, in addition to the discussed parameters the corotating/counterrotating orbits of plasmas, the mass ratio between the binaries, accretion rate, density/temperature profiles, etc. will play

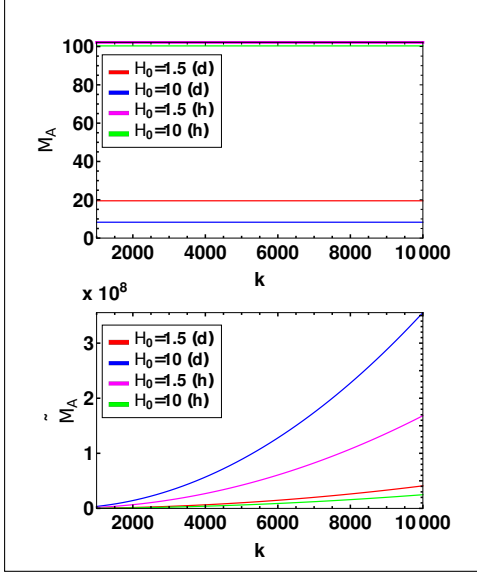


Fig. 7 Alfvén Mach numbers versus k for: macro-scale vector-fields M_A (top) and micro-scale vector-fields \tilde{M}_A (bottom), respectively for generated velocity and magnetic fluctuations for the root 1 of Fig.6; $a = 10$. Bigger the k bigger is \tilde{M}_A while macro-scale velocity fields are practically independent of k for the same H_0 ; generated macro(micro) flows are strongly super-Alfvénic for both fluids (red, blue - degenerate, magenta, green - hot) - Unified Reverse Dynamo/Dynamo scenario.

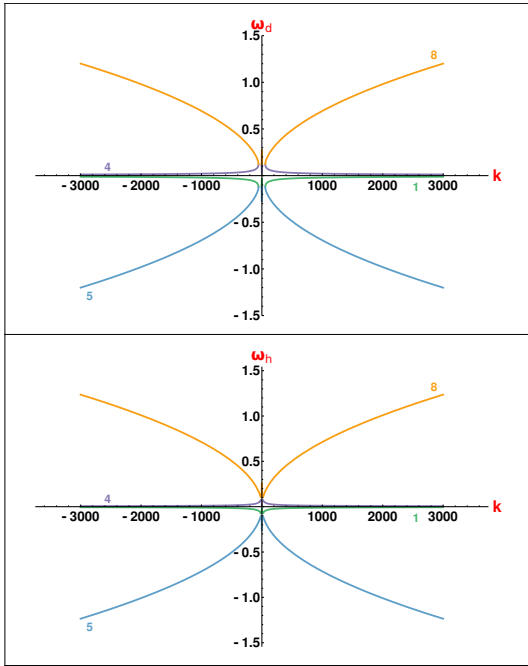


Fig. 8 Solution of dispersion relations (18) (degenerate electron flow - top) and (A5) (relativistically hot flow - bottom) for the (ii-2) case: $a_d = \frac{1}{a_h} \equiv a = 2.45$ - entire ambient system is magnetically dominant; $G_0 = 1.5$, $H_0 = 10$ (solutions show similar picture for $H_0 = 1.5$); 4 different real roots at $q' \simeq q$ are displayed by different color.

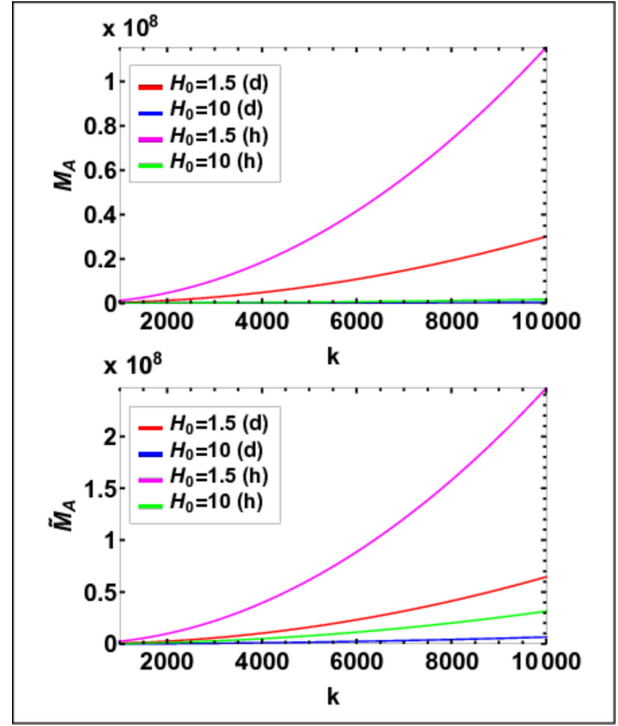


Fig. 9 Alfvén Mach numbers versus k for: macro-scale vector-fields M_A (top) and micro-scale vector-fields \tilde{M}_A (bottom), respectively for generated velocity and magnetic fluctuations for the roots 8 of Fig.8; $a = 2.45$. Bigger the k bigger are both fluids' M_A and \tilde{M}_A ; both macro- and micro-scale velocity fields are strongly super-Alfvénic for both fluids ($\gtrsim 10^8$) - manifestation of perfect Unified Reverse Dynamo/dynamo scenario in both scales (the hot flow M_A -s and \tilde{M}_A -s are multiplied by 10^{-2} for best illustration).

significant role [see e.g. (Rosswog 2015; Liu et al 2017; Figueira et al 2018) for the extensive SPH simulations of the compact objects/binary accreting system global dynamics].

4 Conclusions

From an analysis of relativistic 2-Temperature electron plasma (bulk degenerate e-i fluid with a small fraction of relativistically hot e-i, e.g. like in White Dwarfs accreting hot astrophysical flow / Binary systems) we have extracted the acceleration / generation / amplification of the macro-scale flow/outflow and magnetic field due to Unified Reverse Dynamo/Dynamo Mechanism in the composite astrophysical systems with initial turbulent (micro-scale) magnetic/velocity fields. This process is simultaneous with and complementary to the micro-scale unified D/RD or RD/D dynamics like in two-fluid cases - consequence of magneto-fluid coupling. Generation of macro-scale fast flows (in both degenerate and hot fluids) and strong magnetic fields are simultaneous: the greater the macro-scale magnetic field (generated locally) the greater becomes the macro-scale velocity field (generated locally). Principle results are following:

- Both bulk degenerate fluid and hot contamination undergo the Unified RD/D dynamics; final picture is complex leading to acceleration/amplification of both fluid velocity/magnetic fields.
- Bulk as well and fraction component flow/outflow acceleration and magnetic field amplification due to the Unified RD/D is directly proportional to initial turbulent kinetic or/and magnetic energy in 2-temperature e-i relativistic astrophysical plasma; such flows/magnetic fields are fed by either initial turbulent state: fully kinetically or magnetically dominated ambient system or the different combinations for different fluids. The generated/accelerated outflows are extremely strong when both fluids are magnetically dominant; hot outflows are several orders stronger than the degenerate ones.
- Along with degeneracy level ($G_0(n)$) of bulk system and temperature of a hot fraction (H_0) the scenarios are different for different Beltrami parameters (a_d, a_h) but there always exists such a real $\omega_d(\omega_h)$ (solution of corresponding fluid DR) for which the generation of fast macro-scale locally Super-Alfvénic outflow in one of the fluids or in both fluids or/and the strong macro-scale magnetic field is guaranteed.
- Formation process is less sensitive to hot fluid fraction parameter $\alpha \ll 1$ but more sensitive to its temperature and the corresponding solution of DR - for

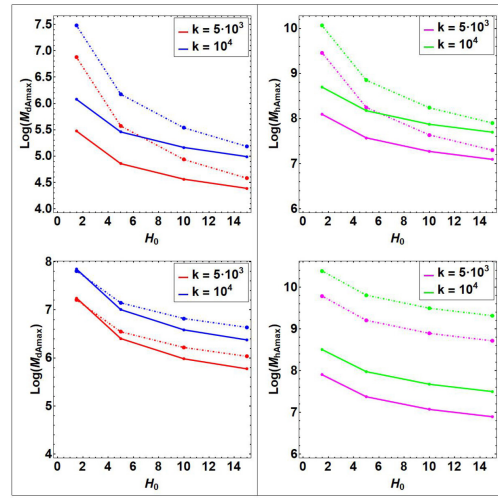


Fig. 10 Maximal values of Alfvén Mach Numbers versus H_0 for: macro-scale vector-fields M_{Amax} (top) and micro-scale vector-fields \tilde{M}_{Amax} (bottom), respectively for the roots 8 of Fig.6 (solid lines, $a = 10$) and roots 8 of Fig.8 (dotted lines, $a = 2.5$ - magnetically dominated ambient system). Smaller the H_0 bigger is the M_{Amax} that can reach values $\gtrsim 10^6$ at small k . Red, blue (magenta, green) colors correspond to: $k = 5 \cdot 10^3$; 10^4 , for degenerate (hot) fluid, respectively. Smaller the k bigger is M_{Amax} for the same H_0 . Macro-scale Mach numbers for hot fluid are 2 orders higher than those for degenerate.

small k the real roots of DR define the processes of either straight D or RD; for big k the generation of strong macro-scale fast, locally Super-Alfvénic flow is guaranteed; for the same degeneracy state of the bulk system, fraction ratio and the magneto-fluid coupling (G_0 , α and a_d , a_h), the smaller is fraction temperature (H_0) larger is the corresponding fluid macro(micro)-scale Alfvén Mach number and, hence, generated flow/outflow (magnetic field) will have a dispersion with Velocity (Magnetic) field distribution in (\mathbf{r}, t) - observations show that large-scale astrophysical flows as well as the magnetic fields are very complex with a characteristic evolution in time and space. The generated macro-scale hot outflow is stronger than the degenerate one for all solutions.

- For some regimes of ambient system parameters (magnetically and/or kinetically dominant mixed ambient system case), the growing accelerated flows in both fluids are sub-Alfvénic - scenario leading to strong magnetic field formation that grows as well - this could explain the formation of macro-scale magnetic fields while the envelope phase of star accretion / binary systems / WD evolution.
- Specifically interesting finding comes to fully magnetically dominant ambient system (for both fluids) when major part of its energy is transformed into the extremely fast super-Alfvénic macro-scale outflow energy due to magneto-fluid coupling for all the real roots of dispersion relation; a weak macro-scale magnetic field is generated along with it - this result is entirely due to the 2-temperature character of ambient composite relativistic system; for realistic physical parameters the resulting accelerated generated locally super-Alfvénic flows are extremely fast with Alfvén Mach number $> 10^6$ as observed in a variety of relativistic astrophysical outflows.

Thus, an intrinsic tendency of flow acceleration / magnetic field amplification due to magneto-fluid coupling in multi-temperature multi-component systems guarantees the simultaneous formation of macro-scale fast flows/outflows and strong magnetic fields through the Unified Reverse Dynamo/Dynamo mechanism - one possible root to understand the evolution of accreting astrophysical objects / binaries of different nature - one of the accessible sources to be considered together with other additional formation mechanisms for macro-scale fast flows/outflows as well as the macro-scale magnetic fields (e.g. energy transformations due to catastrophe or waves in which the gravity, density/temperature inhomogeneities, rotation play important role).

5 Acknowledgements

K.K.-s work was partially supported by World Federation of Scientists National Scholarship Programme Geneva, 2020. This work was partially supported by Shota Rustaveli Georgian National Foundation Grant Project No. FR17-391.

6 The Data Availability Statement

The data to support the outcomes of the work are openly available by the authors upon the reasonable request sent to them directly.

References

- Arshilava, E. Gogilashvili, M., Loladze, V., Jokhadze, I., Modrekiladze, B., Shatashvili, N.L. Tevzadze, A.G. J. High Energy Astrophysics **23**, 6 (2019).
- Asenjo, F.A. and Mahajan, S.M. Physica Scripta, **9(1)**, 015001 (2015).
- Balman S. ASR **66**, 5, 1097 (2020).
- Barnaveli, A.A., Shatashvili, N.L. Astrophys Space Sci. **362**, 164 (2017).
- Begelman, M.C., Blandford, R.D., and Rees, M.D. Rev. Mod. Phys. **56** 255 (1984).
- Berezhiani, V.I., Shatashvili, N.L. and Mahajan, S.M. Phys. Plasmas **22**, 022902 (2015).
- Berezhiani, V.I. and Mahajan, S.M. Phys. Rev. Lett. **73**, 1110 (1994); Phys. Rev. E **52** 1968 (1995).
- Berezhiani, V.I., Mahajan, S.M. and Shatashvili, N.L. Phys. Rev. **A81**, 053812 (2010); *ibid.* J. of Plasma Phys. **76**, 467 (2010).
- Beskin V. S., Phys.-Usp., **53**, 1199 (2010).
- Bhattacharjee, C., Das, R., Stark, D., Mahajan, S.M. Phys. Rev. E, **P92(6)**, 063104 (2015).
- Braithwaite, J., Spruit, H, Nature, **431**, 819 (2004). DOI:10.1038/nature02934
- Briggs, G.P., Ferrario, L., Tout, C.A., Wickramasinghe, D.T., Hurley, J.R. Mon. Not. R. Astron. Soc., **447(2)**, 21, 1713 (2015).
- Camenzind. M. Compact objects in astrophysics: white dwarfs, neutron stars and black holes, Astronomy and astrophysics library. Berlin: Springer-Verlag, (2007).
- Cowling T. G., Mon. Not. R. Astron. Soc., **105**, 166, (1945).
- Ferrario, L., de Martino, D., & Gaensicke, B. T. SSRv, **191**, 111 (2015).
- Ferrario L., Wickramasinghe D.T., Kawka A., ASR, **66**, 5 1025-1056, (2020).
- Figueira, J., José, J., García-Berro, E. Campbell, S. W., García-Senz, D. & Mohamed, S. **A&A**, **613**, A8 (2018). DOI:10.1051/0004-6361/201731545 .
- García-Berro, E., Lorén-Aguilar, P., Aznar-Siguán, G., et al. Astrophys. J., **749**, 25 (2012).
- Hollands, M., Gaensicke, B., & Koester, D. Mon. Not. R. Astron. Soc., **450**, 68 (2015).

- Ji, S., Fisher, R.T, García-Berro, E., Tzeferacos, P., Jordan, G. *Astrophys. J.*, **773**, 136 (2013)
- Kafka, S. & Honeycutt, R.K. *Astrophys. J.*, **128**, 2420 (2004).
- Kawka, A., Vennes, S., Schmidt, G. D., Wickramasinghe, D. T., & Koch, R. *Astrophys. J.*, **654**, 499 (2007).
- Kawka, A. and Vennes, S. *MNRAS* **439**, L90 (2014).
- Kepler, S. O., Pelisoli, I., Jordan, S., Kleinman, S.J., Koester, D., Külebi, D.B., Pecanha, B.V., Castanheira, B.G., Nitta, A., Costa, J.E.S., Winget, D.E., Kanaan, A. and Fraga, L. *Mon. Not. R. Astron. Soc.*, **429**, 2934 (2013).
- Kissin, Y., & Thompson, C. *Astrophys. J.*, **809**, 108 (2015).
- Koester, D. and Chanmugam, G. *Rep. Prog. Phys.* **53**, 837 (1990).
- Kotorashvili, K., Revazashvili, N., Shatashvili, N.L. *AAS*, **365**, 175 (2020).
- Krishnan, V. Venkatraman, Bailes, M., Van Straten, W., Wex, N, Freire, P.C.C., Keane, E.F., Tauris, T.M, Rosado, P.A., Bhat, N.D.R., Flynn, C., Jameson, A. & Osłowski, S. *Science* **367(6477)**, 577 (2020).
- Kryvdyk, V. *Mon. Not. R. Astron. Soc.*, **309**, 593 (1999).
- Kryvdyk, V and Agapitov, A. 15th European Workshop on White Dwarfs. ASP Conference Series, **372**, 411 (2007).
- Külebi, B., Jordan, S., Euchner, F., Gansicke, B. T., & Hirsch, H. *A&A*, **506**, 1341 (2009).
- Liebert, J., Bergeron, P., & Holberg, J. B. *AJ*, **125**, 348 (2003).
- Liebert, J., Bergeron, P., Holberg, J.B. *Astrophys. J. Suppl. Ser.* **156**, 47 (2005).
- Lingam, M., Mahajan, S.M. *Mon. Not. R. Astron. Soc.* **449**, L36 (2015).
- Liu, Z.W., Stancliffe, R.J., Abate, C. and Matroziis, E. *Astrophys. J.*, **846**, 117 (2017).
- Long, K.S., Knigge, C. *Astrophys. J.*, **579**, 725 (2002).
- Mahajan, S.M. and Asenjo, F.A. *Phys. Rev. Lett.*, **107(19)** id. 195003 (2011).
- Mahajan, S.M., Miklaszewski, R., Nikolskaya, K.I. and Shatashvili, N.L. *Phys. Plasmas* **8**, 1340 (2001).
- Mahajan, S.M., Nikolskaya, K. I., Shatashvili, N.L. and Yoshida, Z. *Astrophys. J.* **576**, L161 (2002).
- Mahajan, S.M., Shatashvili, N.L., Mikeladze, S.V. and Sigua, K.I. *Astrophys. J.* **634**, 419 (2005); *Phys. Plasmas* **13**, 062902 (2006).
- Mahajan, S.M. and Lingam, M. *Phys. Plasmas* **22(9)**, 092123 (2015).
- Manfredi, G. *General Relativity and Gravitation* **47(2)**, 1 (2015).
- Mignone, A., Plewa, T. & Bodo, G. *Astrophys. J. Supp.* **160**, 199 (2005).
- Mouchet, M., Bonnet-Bidaud, J.M., de Martino, D. *Mem. SAI* **83**, 578 (2012).
- Mukai, K. *PASP* **129**, 062001 (2017).
- Nordhaus, J., Wellons, S., Spiegel, D.S., Metzger, B.D., Blackman, E.G., Formation of high-field magnetic white dwarfs from common envelopes, *Proceedings of the National Academy of Sciences*, **108(8)**, 3135 2010.
- Ohsaki, S., Shatashvili, N.L., Yoshida, Z. and Mahajan, S.M. *Astrophys. J.* **559**, L61 (2001); *Astrophys. J.* **570**, 395 (2002).
- Oliveira, S.R. and Tajima, T. *Phys. Rev. E* **52**, 287 (1995).
- Puebla, R.E., Diaz, M.P., Hillier, D.J., Hubeny, I. *Astrophys. J.*, **736**, 17 (2011).
- Rosswog, S. *Living Rev. Comput. Astrophys.*, **1**, 1 (2015).
- Ruderman, M.A., & Sutherland, P.G. *NPhS*, **246**, 93 (1973).
- Ryu, D., Chattopadhyay, I & Choi, E. *J. Korean Phys. Soc.* **49(4)**, 1842 (2006).
- Shatashvili, N.L., Mahajan, S.M. and Berezhiani, V.I. *Astrophys. Space Sci.* **361**, 70 (2016).
- Shatashvili, N.L., Mahajan, S.M., Berezhiani, V.I. *Astrophys. Space Sci.* **364**, 148 (2019).
- Shatashvili, N.L., Mahajan, S.M. & Berezhiani, V.I. *Phys. Plasmas*, **27(1)**, 012903 (2020).
- Shatashvili, N.L. and Yoshida, Z. *AIP Conf. Proc.* **1392**, 73 (2011).
- Tremblay, P.-E., Fontaine, G., Freytag, B., Steiner, O., Ludwig, H.-G., Steffen, M., Wedemeyer, S. and Brassard, P. *Astrophys. J.*, **812**, 19 (2015).
- Tout C.A, Wickramasinghe D.T., Liebert J, Ferrario L. and Pringle J.E. *Mon. Not. R. Astron. Soc.* **387**, 897 (2008).
- Tutukov, A.V. and Cherepashchuk, A.M. *Phys.-Usp.* **63**, 209 (2020).
- Warner, B., Cataclysmic variable stars. *Cambridge Astrophysics Series* 28. (1995).
- Wickramasinghe D.T., Ferrario L., *PASP*, **112**, 873 (2000).
- Winget, D.E. and Kepler, S.O. *Annu. Rev. A&A* **46**, 157 (2008).

A Appendix - Derivation of Unified Dynamo/RD relations for relativistically hot fluid fraction

Following the similar procedure as used for degenerate fluid we derive the equations for hot relativistic fluid fraction velocity field (below \mathbf{Q}_h and \mathbf{S}_h are functions of \mathbf{U}_h and \mathbf{B} , as well as plasma-system parameters):

$$m \frac{\partial \tilde{\mathbf{b}}}{\partial t} + m_1 \frac{\partial}{\partial t} \nabla \times \nabla \times \tilde{\mathbf{b}} = (\mathbf{Q}_h \cdot \nabla) \mathbf{b}_0, \quad m \frac{\partial \tilde{\mathbf{v}}_h}{\partial t} + q_1 \frac{\partial}{\partial t} \nabla \times \tilde{\mathbf{b}} = (\mathbf{S}_h \cdot \nabla) \mathbf{b}_0, \quad (\text{A1})$$

$$\text{and} \quad \frac{G_0}{\alpha} \left(G_0 + \frac{H_0}{\alpha} \right) \nabla \times \ddot{\mathbf{B}}, + \left(G_0 + \frac{H_0}{\alpha} \right)^2 \ddot{\mathbf{U}}_h = q_h \nabla \times \mathbf{B} + s_h \nabla \times \mathbf{U}_h, \quad (\text{A2})$$

$$\frac{G_0 H_0}{\alpha} \left(G_0 + \frac{H_0}{\alpha} \right) \nabla \times \nabla \times \ddot{\mathbf{B}} + \left(G_0 + \frac{H_0}{\alpha} \right)^2 \ddot{\mathbf{B}} = r_h \nabla \times \mathbf{B} + p_h \nabla \times \mathbf{U}_h, \quad (\text{A3})$$

$$m_1 \nabla \times \nabla \times \ddot{\mathbf{B}} + m \ddot{\mathbf{B}} = r_h \nabla \times \mathbf{B} + p_h \nabla \times \mathbf{U}_h, \quad q_{1h} \nabla \times \ddot{\mathbf{B}} + m \ddot{\mathbf{U}}_h = q_h \nabla \times \mathbf{H} + s_h \nabla \times \mathbf{U}_h. \quad (\text{A4})$$

This time Dispersion relation reads as follows:

$$\omega_h^8 m'^2 m^2 - \omega_h^4 k^2 \left(2m' m p_h q'_h + m^2 r_h^2 + m'^2 s_h^2 \right) + (p_h q'_h - r_h s_h)^2 k^4 = 0 \quad (\text{A5})$$

$$\text{and} \quad \mathbf{U}_h = \frac{q'_h \left(\omega^4 m' m - (p_h q'_h - r_h s_h) k^2 \right)}{\omega^4 m^2 r_h + s_h (p_h q'_h - r_h s_h) k^2} \mathbf{B}, \quad (\text{A6})$$

$$\text{where} \quad q_{1h} = \frac{G_0}{\alpha} \left(G_0 + \frac{H_0}{\alpha} \right) \equiv \frac{G_0}{H_0} q_1, \quad q'_h = (q_h + q_{1h} \omega^2), \quad \text{as before } m' = (m + m_1 k^2) \text{ and}$$

$$r_h = \alpha \frac{\lambda b_0^2}{3} \left[-\frac{(H_0 - G_0)}{\alpha^2} - \frac{G_0 H_0 \lambda (\chi_h + \lambda)}{\alpha^2} + \alpha \left(\frac{(H_0 - G_0) \chi_h}{\alpha} + \frac{H_0}{\alpha^2} \lambda \right)^2 \right],$$

$$p_h = -\alpha \frac{\lambda b_0^2}{3} \left(-\frac{(H_0 - G_0)}{\alpha} - \frac{G_0 H_0 \lambda (\chi_h + \lambda)}{\alpha} \right).$$

$$\cdot \left[-\frac{(H_0 - G_0)}{\alpha \lambda} - \frac{G_0 H_0 (\chi_h + \lambda)}{\alpha} + \lambda G_0 - \alpha \chi_h \left(\frac{H_0}{\alpha^2} - G_0 \right) - (H_0 - G_0) \chi_h + \frac{H_0}{\alpha} \lambda \right],$$

$$q_h = -\alpha \frac{\lambda b_0^2}{6} \left[\left(\frac{(H_0 - G_0) \chi_h}{\alpha} + \frac{H_0}{\alpha^2} \lambda \right) \xi_{1h} - \frac{\lambda G_0}{\alpha^2} + \frac{\chi_h}{\alpha} \left(\frac{H_0}{\alpha^2} - G_0 \right) \right],$$

$$s_h = -\alpha \frac{\lambda b_0^2}{6} \left[\left(\lambda \frac{G_0}{\alpha} - \chi_h \left(\frac{H_0}{\alpha^2} - G_0 \right) \right) \left(\frac{1}{\alpha \lambda} + \lambda G_0 - \alpha \chi_h \left(\frac{H_0}{\alpha^2} - G_0 \right) \right) - \left(\frac{(H_0 - G_0)}{\alpha} + \frac{G_0 H_0 \lambda (\chi_h + \lambda)}{\alpha} \right) \xi_{1h} \right] \quad (\text{A7})$$

with

$$\xi_{1h} = \left(\frac{(1 + 2G_0 \lambda^2 - 2G_0^2 \eta' \lambda^2)}{\alpha} - 2G_0 (G_0 \eta' - 1) \lambda \chi_h + \frac{G_0 \eta' (H_0 \lambda (\chi_h - \lambda) - 1)}{\alpha^2} \right), \quad \eta' = \frac{G_0}{\alpha q_{1h}}. \quad (\text{A8})$$

For small \mathbf{k} leading to $m' = m$, $q' = q$ and for dispersion we have:

$$\omega_h^8 m^4 - \omega_h^4 k^2 m^2 \left(2p_h q_h + r_h^2 + s_h^2 \right) + (p_h q_h - r_h s_h)^2 k^4 = 0, \quad (\text{A9})$$

$$\text{with} \quad \omega_{h1(2)}^4 = \frac{k^2}{2m} \left(2p_h q_h + r_h^2 + s_h^2 \pm (r_h + s_h) \sqrt{(r_h - s_h)^2 + 4p_h q_h} \right) \quad (\text{A10})$$

and consequently the relation between fields is:

$$\mathbf{U}_h = \frac{s_h - r_h \pm \sqrt{4p_h q_h + (r_h - s_h)^2}}{2p_h} \mathbf{B} . \quad (\text{A11})$$